J|A|C|S
ARTICLES
Published on Web 06/25/2005

Energy Funneling of IR Photons Captured by Dendritic Antennae and Acceptor Mode Specificity: Anti-Stokes Resonance Raman Studies on Iron(III) Porphyrin Complexes with a Poly(aryl ether) Dendrimer Framework

Yu-Jun Mo,[†,§] Dong-Lin Jiang,[‡] Makoto Uyemura,[‡] Takuzo Aida,[‡] and Teizo Kitagawa*[,†]

Contribution from the Okazaki Institute for Integrative Bioscience, National Institutes of Natural Sciences, Myodaiji, Okazaki 444-8787, Japan, and Department of Chemistry and Biotechnology, School of Engineering, The University of Tokyo, Hongo, Bunkyo-ku, Tokyo 113-8656, Japan

Received December 28, 2004; E-mail: teizo@ims.ac.jp

Abstract: A series of poly(aryl ether) dendrimer chloroiron(III) porphyrin complexes (L_nTPP)Fe(III)Cl (number of aryl layers [n] = 3 to 5) were synthesized, and their Boltzmann temperatures under IR irradiation were evaluated from ratios of Stokes to anti-Stokes intensities of resonance Raman bands. While the Boltzmann temperature of neat solvent was unaltered by IR irradiation (L_nTPP)Fe(III)Cl (n = 3 to 5), all showed a temperature rise that was larger than that of the solvent and greater as the dendrimer framework was larger. Among vibrational modes of the metalloporphyrin core, the temperature rise of an axial Fe−Cl stretching mode at 355 cm^{-1} was larger than that for a porphyrin in-plane mode at 390 cm^{-1}. Although most of the IR energy is captured by the phenyl ν_8 mode at 1597 cm^{-1} of the dendrimer framework, an anti-Stokes Raman band of the phenyl ν_8 mode was not detected, suggesting the extremely fast vibrational relaxation of the phenyl mode. From these observations, it is proposed that the energy of IR photons captured by the aryl dendrimer framework is transferred to the axial Fe−Cl bond of the iron porphyrin core and then relaxed to the porphyrin macrocycle.

Introduction

Biological photosynthesis, which converts solar energy into chemical potentials, is a critical photochemical event in plants. In purple photosynthetic bacteria, for example, wheel-like arrays of bacteriochlorophyll units play a key role in the efficient capture of light energy and its subsequent funneling into the reaction center.[1] This structural feature has motivated chemists to design artificial light-harvesting antennae and to explore their photochemical properties for the purpose of realizing long-range vectorial energy transfers. Since the first report of Balzani and co-workers on photophysical properties of ruthenium(II)/osmium(II) multinuclear supramolecular dendrimers,[2] dye-functionalized dendritic macromolecules have attracted great attention as light-harvesting antennae for energy transduction.[3] Due to the flexibility of molecular design, dendritic architectures allow site-specific positioning of multiple chromophore units in a three-dimensional nanospace. Examples of pioneering works include photochemical studies on dendritic macromolecules such as self-assembled lanthanide-core dendrimers,[4] perylene-terminated phenylacetylene conjugated dendrons,[5] and porphyrin-incorporated dendrimers,[6] along with some theoretical calculations on energy transfer events in dendritic macromolecules.[7]

Through studies on a series of porphyrin-cored poly(benzyl ether) dendrimers and dendrons, we have found that a large, spherical fourth-generation dendrimer porphyrin, upon exposure to UV light, shows an exceptionally high energy transfer efficiency from the peripheral aromatic units to the porphyrin core.[6c] An analogous trend has been observed for star and conically shaped dendritic zinc porphyrin arrays having a free-base porphyrin core, where the former shows a much more

† National Institutes of Natural Sciences.
‡ The University of Tokyo.
§ Present address: Physics Department, Henan University, Kaifeng 475001, China. E-mail: yujunmo@henu.edu.cn.

(1) Mcdermott, G.; Prince, S. M.; Freer, A. A.; Hawthornthwaite-Lawless, A. M.; Rapiz, M. Z.; Cogdell, R. J.; Isaacs, N. W. *Nature* **1995**, *374*, 517−521.
(2) Campagna, S.; Denti, G.; Serroni, S.; Ciano, M.; Juris, A.; Balzani, V. *Inorg. Chem.* **1992**, *31*, 2982−2984.
(3) For selected reviews, see: (a) Aida, T.; Jiang, D.-L. In *Dendrimers and Dendritic Polymers*; Fréchet, J. M. J., Tomalia, D. A., Eds.; Wiley-VCH: Weinheim, Germany, 2000; Chapter 17, pp 425−438. (b) Adronov, A.; Fréchet, J. M. J. *Chem. Commun.* **2000**, 1701−1710. (c) Choi, M.-S.; Yamazaki, T.; Yamazaki, I.; Aida, T. *Angew. Chem., Int. Ed.* **2004**, *43*, 150−158.
(4) Kawa, M.; Fréchet, J. M. J. *Chem. Mater.* **1998**, *10*, 286−296.
(5) (a) Devadoss, C.; Bharathi, P.; Moore, J. S. *J. Am. Chem. Soc.* **1996**, *118*, 9635−9644. (b) Kopelman, P.; Shortreed, M.; Shi, Z.-Y.; Tan, W.; Xu, Z.; Moore, J. S.; Klafter, J. *Phys. Rev. Lett.* **1997**, *78*, 1239−1242.
(6) (a) Aida, T.; Jiang, D.-L. In *The porphyrin handbook Vol. 3. Inorganic, Organometallic, and Coordination Chemistry*; Kadish, K. M., Smith, K. M., Guilard, R., Eds.; Academic Press: New York, 2000; pp 369−384. (b) Jin, R.-H.; Aida, T.; Inoue, S. *J. Chem. Soc., Chem. Commun.* **1993**, 1260−1261. (c) Jiang, D.-L.; Aida, T. *J. Am. Chem. Soc.* **1998**, *120*, 10895−10901. (d) Choi, M.-S.; Aida, T.; Yamazaki, T.; Yamazaki, I. *Angew. Chem., Int. Ed.* **2001**, *40*, 3194−3198. (e) Choi, M.-S.; Aida, T.; Yamazaki, T.; Yamazaki, I. *Chem.−Eur. J.* **2002**, *8*, 2668−2673.
(7) (a) Bar-Haim, A.; Klafter, J.; Kopelman, R. *J. Am. Chem. Soc.* **1997**, *119*, 6197−6198. (b) Tretiak, S.; Chernyak, V.; Mukamel, S. *J. Phys. Chem. B* **1998**, *102*, 3310−3315.

10.1021/ja042196z CCC: $30.25

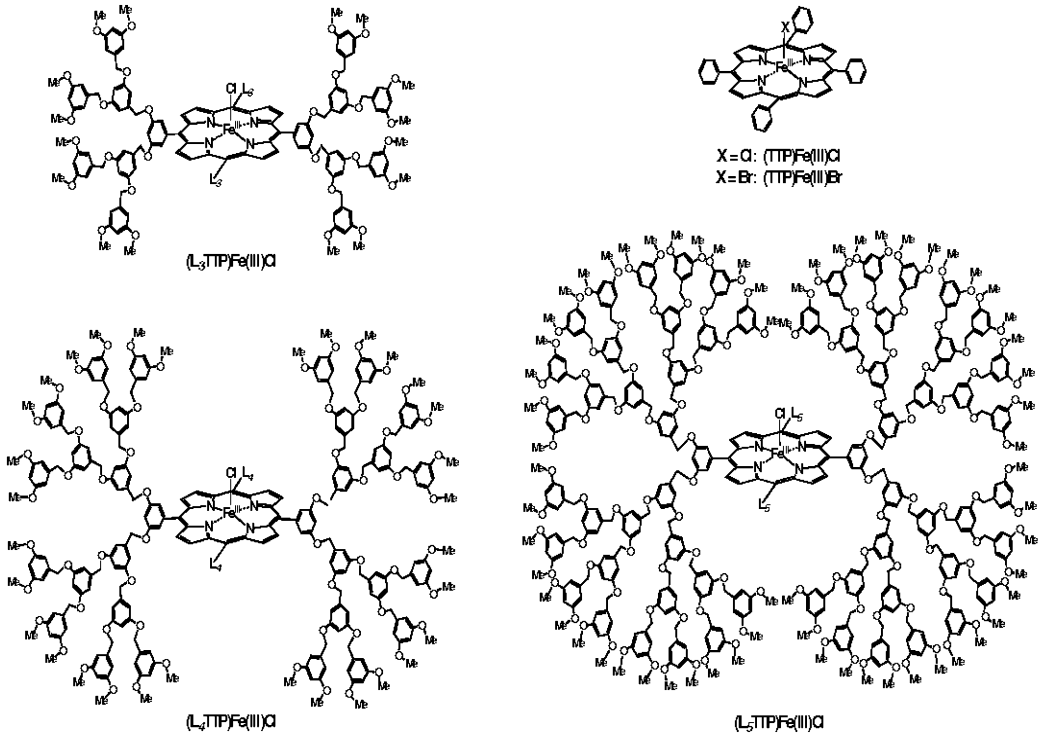

Figure 1. Schematic representations of (TPP)Fe(III)X (X = Cl or Br) and (L_nTPP)Fe(III)Cl (n = 3 to 5).

efficient energy transfer than the latter upon visible-light excitation of the peripheral zinc porphyrin units.[6d,e] These observations, along with fluorescence anisotropy studies, have indicated a morphology effect on the light-harvesting functions of dendritic macromolecules. In relation to such antenna effects of dendrimers for UV and visible lights, we have reported an intriguing phenomenon that large third- and fourth-generation poly(benzyl ether) dendrimers with an azobenzene core, upon exposure to infrared (IR) light, undergo cis-to-trans isomerization of the azobenzene unit.[8] A detailed study with monochromatized IR lights has indicated that the energy of IR photons absorbed by the aromatic building units in the dendrimer framework is responsible for this isomerization. Among three different wavenumbers used for IR irradiation [2500 cm^{-1} (transparent), 1597 cm^{-1} (ν_8), and 1155 cm^{-1} (CH_2-O str.)], only the 1597 cm^{-1} radiation facilitated the isomerization reaction, and the observed dependence of the isomerization rate constant on the IR irradiation intensity indicated that 4.9 photons are involved in this photochemical process of the $n = 5$ azodendrimer.[8] Under otherwise identical conditions, lower-generation homologues as well as nondendritic azobenzene did not show any response to IR irradiation. We have tentatively suggested that a large poly(benzyl ether) dendrimer framework around the azobenzene core could prevent the vibrational energy from dissipation, whereas such an energy dissipation in ordinary systems takes place instantaneously.

In the present work, we synthesized poly(benzyl ether) dendrimers (L_nTPP)Fe(III)Cl (Figure 1; number of benzyl ether layers; n = 3 to 5) bearing a chloroiron(III) porphyrin functionality at the core and investigated their Raman spectral features in dioxane under irradiation with IR light that can excite the aromatic units in the dendrimers. Since the porphyrin core undergoes no photochemical reaction under IR irradiation, it enabled us to repeat the phenomenon for an identical sample and thus to accumulate the spectra to raise the signal-to-noise ratios. It is well established that the intensity of anti-Stokes Raman scattering reflects the Boltzmann temperature because the scattering intensity is proportional to the population at vibrationally excited levels. Even if an absolute value of a scattering cross section is not available, the Boltzmann temperature can be determined from the ratio of the Stokes Raman intensity (I_S) to the anti-Stokes Raman intensity (I_{AS}) of a given vibrational mode. By means of picosecond time-resolved anti-Stokes Raman scattering spectroscopy, we have successfully analyzed the cooling process of heme following photodissociation of CO from carbonmonoxy-myoglobin.[9]

Given the validity of this method, we herein applied continuous wave (CW) anti-Stokes Raman spectroscopy to (L_nTPP)-Fe(III)Cl (n = 3 to 5) for the investigation of energy funneling of IR photons captured by their dendritic antennae. (L_nTPP)-Fe(III)Cl (n = 3 to 5) under IR illumination could enable monitoring of the Boltzmann temperatures of their individual building units. One may argue against this possibility because the vibrational relaxation is so fast that stationary-state measurements would not provide any correct information. This would be true if the number of IR capturing units is small. When this number is sufficiently large, IR energy captured by different antenna units at the same time increases and may exceed the relaxation rate at the porphyrin, although a nonlinear relaxation process such as annihilation may provide additional pathways compared to lower generation dendrimers. As a result, it may practically raise the temperature of the porphyrin core during IR irradiation. Indeed, the results with higher-generation (L_n-TPP)Fe(III)Cl clearly indicated that the energy acquired from IR light is localized to a great extent at the focal Fe−Cl bond. In the present article, we report effects of IR irradiation on

(8) Jiang, D.-L.; Aida, T. *Nature* **1997**, *388*, 454−456.

(9) Mizutani, Y.; Kitagawa, T. *Science* **1997**, *278*, 443−445.

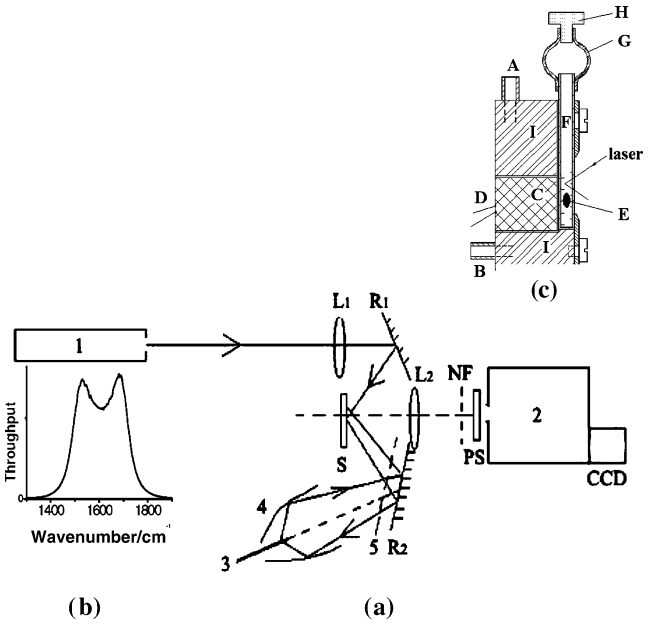

Figure 2. Schematic diagram of the system for Raman measurements under IR illumination. (a) Scheme for the whole measurement system. **1**, laser; **2**, polychromator for Raman spectra; **3**, ceramic heater as an IR source; **4**, ellipsoidal reflecting mirror; **5**, IR band-pass filter; **L1** and **L2**, focusing lenses; **R1**; laser reflection mirror; **R2**, gold-coated IR reflection mirror; **S**, CaF_2 sample cell; **NF**, notch filter; **PS**, polarization scrambler. (b) Transmission spectrum of the IR band-pass filter in the 1300−1900 cm^{-1} range, while more details are given in Figure S3. (c) The rectangular CaF_2 sample cell and cell holder. **A**, inlet of circulating water from the temperature-controlling equipment; **B**, outlet for circulating water; **C**, magnetic mixer driver; **D**, power supply for the magnetic mixer; **E**, magnetic stir bar; **F**, rectangular CaF_2 cell; **G**, glass transfer; **H**, Teflon stopper; **I**, copper block.

intensity ratios of Stokes and anti-Stokes Raman bands of (L_n-TPP)Fe(III)Cl (n = 3 to 5) and compare the Boltzmann temperatures of the Fe−Cl bond, porphyrin macrocycle, and dendritic aromatic units, in comparison with that of dioxane as the solvent.

Experimental Section

Preparation of Samples. (L_nTPP)Fe(III)Br (n = 3 to 5) was synthesized as previously described.[10] Briefly, a tetrahydrofurane (THF) solution containing free-base (L_nTPP)H_2 and $FeBr_2$ (2−10 equiv) was refluxed under Ar for 18 h. Completion of metal insertion was assessed by following the change in the UV−visible spectrum for the disappearance of fluorescence from (L_nTPP)H_2. The reaction mixture was chromatographically separated on silica gel using $CHCl_3$ as the eluent. The second fraction collected was put into methanolic HCl (0.1 M). The (L_nTPP)Fe(III)Cl thus prepared was recrystallized from a $CHCl_3$/MeOH mixture. Dioxane solutions of (L_nTPP)Fe(III)Cl were used at a concentration of approximately 2×10^{-4} M for Raman spectroscopy.

(TPP)Fe(III)Cl was purchased from Aldrich Chemical Co. (TPP)-Fe(III)Br was synthesized from (TPP)Fe(III)Cl via [(TPP)Fe(III)]$_2$O, by mixing 5 mg of (TPP)Fe(III)Cl in 50 mL of CH_2Cl_2 with 50 mL of 1 M aqueous NaOH solution, followed by addition of 50 mL of 1 M aqueous HBr. The CH_2Cl_2 layer of the resulting mixture was collected by a separatory funnel and evaporated to give (TPP)Fe(III)Br.

Raman Measurements. Figure 2a schematically illustrates our Raman measurement-IR irradiation system. Raman scattering was excited by the 413.1-nm line of a Kr^+ ion laser (Figure 2a; **1**), and the scattered light from the sample (**S**) was collected by an objective lens (**L2**) into a polychromator (**2**) equipped with liquid nitrogen-cooled charge-coupled device (CCD) as a detector. The laser power at the sample point was 3 mW, unless otherwise stated. The measurements of the ratios of Stokes and anti-Stokes Raman intensities of a solvent band of sample solutions with the laser power of 3 mW indicated that the temperature was 1.5 K higher than the case with 0.6 mW (lowest power) even when water at 21 °C was circulated through the cell holder. Accordingly, the surrounding temperature for the dendrimer samples in the practical measurements was 22.5 °C.

The source of IR irradiation (**3**), which is a ceramic heater of 60 W (Jasco, model LS-600), is expected to emit radiation close to the blackbody at 1300 °C at 100 V of applied voltage. The real emission pattern from the ceramic heater in the 4000−1000 cm^{-1} region measured with an FTIR spectrometer is given in Figure S1 in the Supporting Information. The temperature of the heater, but not the IR intensity, is linearly proportional to the applied AC voltage between 75 and 110 V. This IR source was placed at one of the focal points of an ellipsoidal mirror (**4**; Hamamatsu Photonics, model E4169-01), and the sample was placed at the other focal point using a reflection mirror (**R2**) to conduct the IR radiation effectively onto the sample. To see qualitative effects of IR irradiation intensity on the Boltzmann temperatures, the output intensity of the IR source was changed by varying the input electric (AC) voltage to the ceramic heater.

The band-pass filter (**5**; Jasco, model 6.275 μm) was placed when necessary. This filter transmits IR light between 1730 and 1480 cm^{-1} with a transmittance of 50−100% but <1% in the 8000−1900 and 1400−1100 cm^{-1} regions. Its transmittance spectrum observed in this study is illustrated by Figure 2b, and the more detailed spectrum between 8000 and 350 cm^{-1} is given in the Supporting Information (Figure S2). The transmittance at 1597 cm^{-1} is 70.05%.

As illustrated in Figure 2c, the sample cell, which was designed specifically for this study, is a rectangular cuvette (**F**) made of an optical CaF_2 crystal with a cross section of 8×3 mm^2 (inside) and a height of 45 mm. The cuvette is held by a copper holder (**I**), and its temperature is maintained by circulating temperature-controlled water from **A** to **B** through **I** as shown in Figure 2c. A magnetic stirring bar (**E**) was placed in the cuvette and rotated by a mixer (**C**) during the Raman measurements. To examine the performance of this IR irradiation system, we applied it to an azobenzene-containing dendrimer[8] and measured its UV−vis spectrum instead of its Raman spectrum. Its performance was confirmed when we observed that the absorption spectral change due to the cis-to-trans isomerization of azobenzene occurred even at the lowest voltage (55 V) applied to the ceramic heater. Accordingly, the present IR irradiation power at the lowest applied voltage is sufficient to induce the reaction requiring 4.9 IR photons,[8] and it can be increased by raising the applied voltage.

Results

To identify the axial Fe−Cl vibrational mode of (L_nTPP)-Fe(III)Cl, we utilized two nondendritic (TPP)Fe(III)X complexes (Figure 1; X = Cl or Br) as model compounds. Figure 3 displays the low-frequency anti-Stokes resonance Raman spectra of (TPP)Fe(III)X (X = Cl or Br) in CH_2Cl_2 obtained with excitation at 413.1 nm. The band marked with an asterisk arose from the solvent. (TPP)Fe(III)Cl and (TPP)Fe(III)Br did not show any difference in the high-frequency region from 1200 to 1700 cm^{-1} of the Stokes spectra (data not shown) but exhibited a distinct difference in the low-frequency region. The 355-cm^{-1} band of (TPP)Fe(III)Cl (Figure 3a) disappears in the spectrum of (TPP)Fe(III)Br (Figure 3b), but a new band appears at 237 cm^{-1}. These two frequencies are similar to the previously reported Fe−X stretching modes of (OEP)Fe(III)X (OEP = octaethylporphyrin) at 606, 364, and 279 cm^{-1} for X = F, Cl,

(10) (a) Jiang, D.-L.; Aida, T. *Chem. Commun.* **1996**, 1523−1524. (b) Jiang, D.-L.; Aida, T. *J. Macromol. Sci., Pure Appl. Chem.* **1997**, *A34*, 2047−2055.

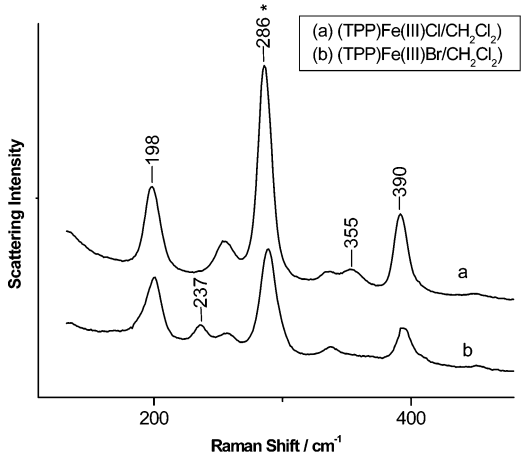

Figure 3. Anti-Stokes resonance Raman spectra of (TPP)Fe(III)X (for a, X = Cl and for b, X = Br) in CH_2Cl_2 at an environmental temperature of 294.2 K and excitation by a Kr^+ ion laser at 413.1 nm with a power of 1 mW.

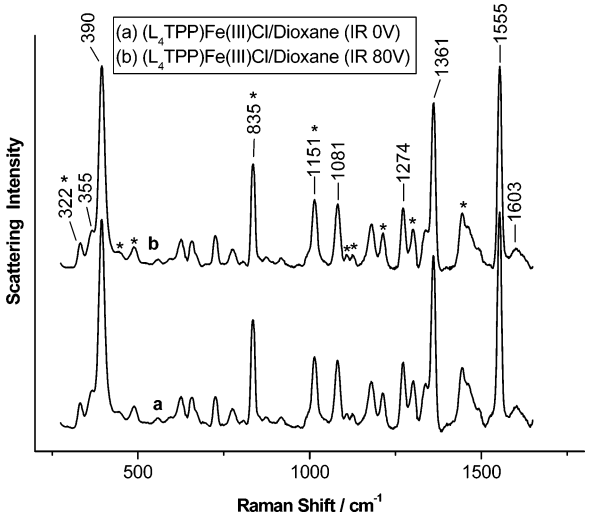

Figure 4. Stokes resonance Raman spectra of L_4(TPP)Fe(III)Cl in dioxane in the absence of IR band-pass filter with a voltage applied to the IR source at (a) 0 V and (b) 80 V at an environmental temperature of 295.7 K and excitation by a Kr^+ ion laser at 413.1 nm with a power of 3 mW. The spectral background was taken out.

and Br, respectively.[11] Accordingly, the 355-cm^{-1} band observed in Figure 3a can be assigned to the axial Fe−Cl stretching mode of (TPP)Fe(III)Cl.

Figure 4 shows the typical Stokes resonance Raman spectra of L_4(TPP)Fe(III)Cl in dioxane in the presence and absence of IR irradiation. The bands marked with an asterisk originate from the solvent, whereas the band at 322 cm^{-1} is due to the CaF_2 cell. Other bands are assigned to modes of (TPP)Fe(III); the detailed analysis of vibrational modes was carried out as described by Spiro and co-workers.[12] The number and positions of peaks in the resonance Raman spectrum remained unchanged after prolonged IR irradiation, even at an applied voltage of 80 V. In good agreement with the assignment established in the model study, in both cases we observed a band at 355 cm^{-1} due to the axial Fe−Cl stretching vibrational mode. On the other hand, a representative porphyrin in-plane vibrational band was

(11) Kitagawa, T.; Abe, M.; Kyogoku, Y.; Ogoshi, H.; Watanabe, E.; Yoshida, Z. *J. Phys. Chem.* **1976**, *80*, 1181−1186.
(12) Li, X.-Y.; Czernuszewicz, R. S.; Kincaid, J.; Su, Y.-O.; Spiro, T. G. *J. Phys. Chem.* **1990**, *94*, 31−47.

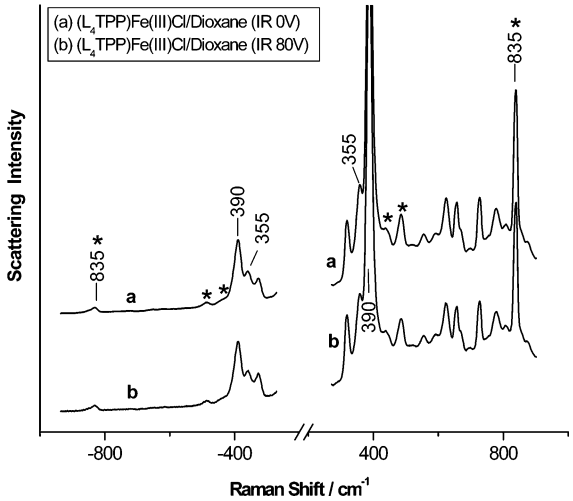

Figure 5. Stokes and anti-Stokes resonance Raman spectra of L_4(TPP)-Fe(III)Cl in dioxane in the absence of an IR band-pass filter with a voltage applied to the IR source at (a) 0 V and (b) 80 V (295.7 K, 413.1 nm, 3 mW).

observed at 390 cm^{-1} (porphyrin ν_8) with relatively high intensity. This mode includes primarily the Fe−N stretching vibration and some contributions from the $C_\alpha-C_m-C_\alpha$ deformation and C_m-C_α stretching.[12] Virtually identical Stokes Raman spectra were observed for lower-generation L_3(TPP)-Fe(III)Cl and higher-generation L_5(TPP)Fe(III)Cl.

Figure 5 shows the simultaneously observed anti-Stokes and Stokes resonance Raman spectra between −950 and +950 cm^{-1} of L_4(TPP)Fe(III)Cl measured with the same experimental conditions as those for Figure 4. (Hereafter, the anti-Stokes region is designated by negative wavenumbers.) The anti-Stokes bands at −355 and −390 cm^{-1}, corresponding to the axial Fe−Cl stretching and porphyrin in-plane vibrational modes, respectively, are clearly observed but with much weaker intensity than those at +355 and +390 cm^{-1}. Spectra a and b reflect the Raman intensities in the absence and presence of IR irradiation, respectively. Their intensities apparently changed little with IR irradiation, but precise analysis demonstrated systematic changes as described later. The anti-Stokes solvent band at −835 cm^{-1} is also discernible. The extended anti-Stokes resonance Raman spectra of L_4(TPP)Fe(III)Cl obtained with the same instrumental conditions are given in the Supporting Information (Figure S3). Anti-Stokes Raman bands corresponding to the high-frequency modes of porphyrin above 1000 cm^{-1} and the aryl ν_8 mode around 1600 cm^{-1} were not observed even when a voltage of 80 V was applied to the ceramic heater.

To determine the vibrational temperature, it is essential to evaluate the area intensities of individual Raman bands correctly. Its adopted procedure is explained in Figure 6, in which the solid and broken lines denote the observed and fitted spectra, respectively. The spectral fitting was performed with the program Grams/32, version 4.14 (Spectral Notebase, Galactic Industries Corp.). When an appropriate spectral range and the number of bands contained therein are given, this program makes a linear base line and fits the spectra with the given number of Lorentzian-Gaussian mixed functions. In practice, as shown in Figure 6, we assumed the presence of a single band in the frequency range between −910 and −760 cm^{-1}, five bands between −540 and −280 cm^{-1}, five bands between +280 and +530 cm^{-1}, and five bands between +700 and +875 cm^{-1}

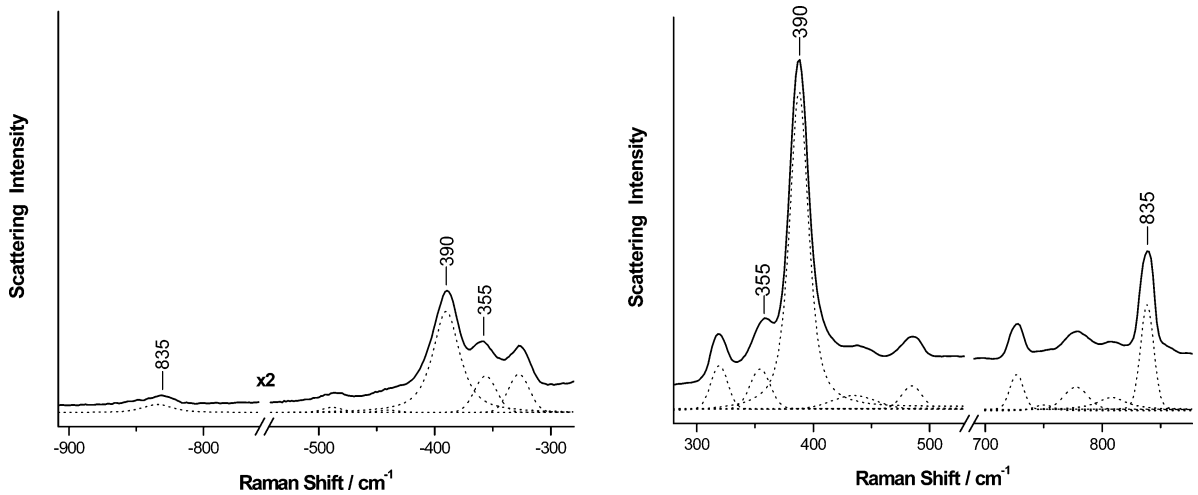

Figure 6. Spectral fitting for Figure 5b with Grams/32, version 4.14 (Galactic Industries Corp.). Solid lines denote the observed spectra (Figure 5b) and broken lines indicate the fitted spectra after subtraction of the computer defined linear base line. The left and right panels represent the anti-Stokes and Stokes spectra, respectively.

to evaluate the band intensities of the bands at −835, −390 and −355, +355 and +390, and +835 cm^{-1}, respectively. The solid lines in Figure 6 denote the corresponding regions of Figure 5b in a discontinuous way, and the broken lines denote the simulated spectra which are represented as baseline subtracted spectra. The area intensities were calculated for three bands thus derived at 355 cm^{-1} (Fe−Cl stretching), 390 cm^{-1} (porphyrin ν_8 mode), and 835 cm^{-1} (solvent). The intensities will be utilized later for the evaluation of their Boltzmann temperatures. For neat solvent, only the 835 cm^{-1} bands were measured under IR irradiation and demonstrated no temperature increase under IR irradiation within the uncertainty of 0.6 °C.

Discussion

Theoretical Base and Practical Data Treatment. The ratio of Stokes (I_S) to anti-Stokes (I_{AS}) Raman intensities for a nondegenerate vibrational mode (ν_i) in a thermal equilibrium at a particular absolute temperature (T) can be represented by the following equation:[13]

$$I_S/I_{AS} = [(\nu_0 - \nu_i)/(\nu_0 + \nu_i)]^3 \exp(h\nu_i/kT) \qquad (1)$$

where ν_0 is the frequency of Raman excitation light, $\nu_0 - \nu_i$ and $\nu_0 + \nu_i$ are the absolute frequencies of Stokes and anti-Stokes Raman bands, respectively, and h and k are Planck's and Boltzmann's constants, respectively. In the physical sense, the intensity ratio of Stokes to anti-Stokes Raman bands depends only on the population ratio of the vibrationally excited to the ground levels. If thermal equilibrium has not been established, vibrational populations among different modes cannot be determined with this equation. However, even in such a case, the vibrational temperature of a given mode can be defined by eq 1, and, therefore, cooling of photoexcited metalloporphyrin was successfully estimated from the temporal dependence of the anti-Stokes Raman intensities.[14] For the sake of convenience, we call such a temperature the Boltzmann temperature, because it may differ from the macroscopic temperature. Accordingly, the Boltzmann temperature (T_w) is defined for each vibrational mode, where w denotes a vibrational frequency (ν_i) and can be obtained experimentally from the I_S/I_{AS} measurement as follows:

$$T_w = (h\nu_i/k)/\ln[(\nu_0 + \nu_i)^3 I_S/(\nu_0 - \nu_i)^3 I_{AS}] \qquad (2)$$

Although the vibrational mode dependence would not be large in the measurements using a CW laser due to rapid vibrational relaxation, some trends are expected to appear if the Fe−Cl bond is specifically heated.

In the case of nonresonance Raman scattering, absorption for scattered light is negligible and, accordingly, the observed intensities would correspond to true intensities. In the case of resonance Raman scattering, however, the absorption of scattered light by the solution is different at $\nu_0 + \nu$ and $\nu_0 - \nu$ in the envelope of absorption band of the solution. This effect is larger as the separation between $\nu_0 + \nu$ and $\nu_0 - \nu$ becomes larger and thus depends on vibrational frequency ν. Furthermore, the scattering cross section under resonance conditions at an excitation frequency ν_0 for Stokes and anti-Stokes Raman scattering are, strictly speaking, different (difference in E_i in the denominator of the scattering cross section). To reduce such effects, we selected smaller values of ν among many Raman bands and two different modes whose ν were close to each other. Since amounts of real absorption for the excitation light and the scattered light by the sample solution depend on the optical pass length through the solution (a distance between the cell surface and scattering point) in each measurement and thus on the geometrical arrangement of the cell, quantitative estimation of these terms is difficult. However, to precisely determine the Boltzmann temperature from the ratio I_S/I_{AS}, such effects should be corrected experimentally as much as possible.

These effects would be the same at different temperatures for a given scattering setting of the sample and for a given vibrational mode. To circumvent these problems, we tried to incorporate these effects into I_S/I_{AS} using a correction factor. The basic assumption is that the experimental I_S/I_{AS} can be represented by the true $(I_S/I_{AS})_{true}$ multiplied with a correction factor, $C_i \times (I_S/I_{AS})_{true}$. The value of C_i depends on vibrational mode and scattering geometry but not on temperature (applied voltage for IR irradiation). In other words, C_i is specific to a given experimental geometry and concentrations of sample and therefore can be used for all temperatures under the same

(13) Kip, B. J.; Meier, R. J. *Appl. Spectrosc.* **1990**, *44*, 707−711.
(14) Mizutani, Y.; Kitagawa, T. *Bull. Chem. Soc. Jpn.* **2002**, *75*, 623−639.

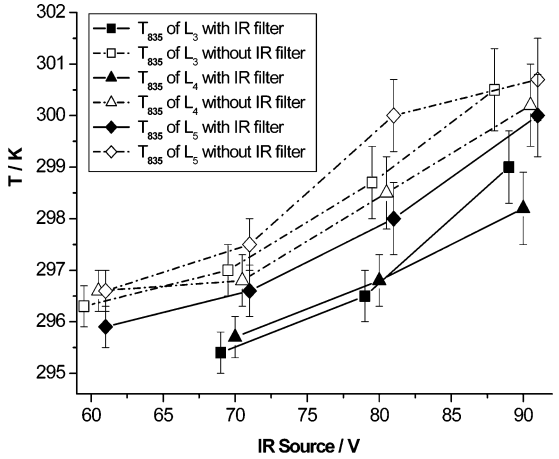

Figure 7. Dependence of the Boltzmann temperatures of the solvent T_{835} in a solution of (L_nTPP)Fe(III)Cl/dioxane on the voltage applied to the IR source. The experiment was performed in the absence (open markers) and presence (filled markers) of an IR band-pass filter at an environmental temperature of 295.7 K and excitation by a Kr^+ ion laser at 413.1 nm with a power of 3 mW.

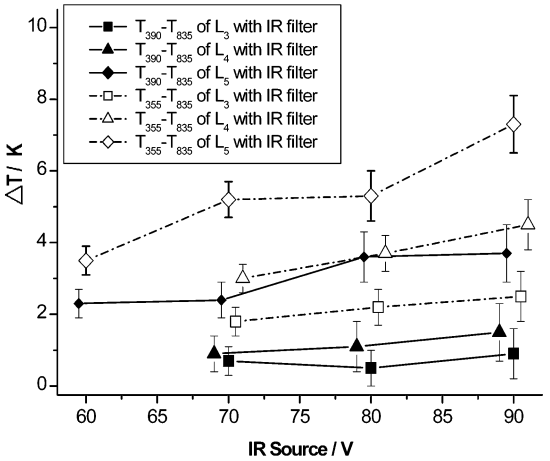

Figure 8. Dependence of the Boltzmann temperatures ΔT_{390} ($T_{390} - T_{835}$) and ΔT_{355} ($T_{390} - T_{835}$) of a (L_nTTP)Fe(III)Cl/dioxane solution on the voltage applied to the IR source in the presence of IR band-pass filter at an environmental temperature of 295.7 K. The complete sets of independent measurements were carried out three, three, and two times for L_3, L_4, and L_5 samples, respectively. The error bars were determined from the scattering of the data.

scattering geometry when C_i is determined at a certain temperature. The true value, $(I_S/I_{AS})_{true}$, would be obtainable for ideal experimental values of I_S and I_{AS} and therefore should be the same value as that obtained from eq 1 when $T = T_0$ and $\nu = \nu_i$.

We determined the value of C_i using the experimental value of I_S/I_{AS} [$= (I_S/I_{AS})_0$] obtained from each Raman measurement of (L_nTPP)Fe(III)Cl at room temperature without IR irradiation and the ideal true value, $(I_S/I_{AS})_{true}$, calculated from eq 1 with ν_i and T_0. Accordingly, C_i was determined for each ν_i:

$$C_i = (I_S/I_{AS})_0/(I_S/I_{AS})_{true} \quad (3)$$

For example, the $(I_S/I_{AS})_{true}$ values for $T = 294.2 + 1.5 = 295.7$ K (22.5 °C) are 47.41, 6.064, and 5.158 for the bands at 835, 390, and 355 cm^{-1}, respectively, and the experimental $(I_S/I_{AS})_0$ values for (L_nTPP)Fe(III)Cl in dioxane in the absence of IR irradiation were 15.13, 5.252, and 2.458 for bands at 835, 390, and 355 cm^{-1}, respectively. Accordingly, the values of C_i are 0.3192, 0.8661, and 0.4765 for the 835, 390, and 355 cm^{-1} bands, respectively. In the practical measurements under IR irradiation, the true value of I_S/I_{AS} is $(I_S/I_{AS})_T$ and the experimentally obtained value of I_S/I_{AS} is $(I_S/I_{AS})_{obs}$. $(I_S/I_{AS})_T$ was obtained from $(I_S/I_{AS})_{obs}$ using the following equation for three kinds of ν_i.

$$(I_S/I_{AS})_T = (I_S/I_{AS})_{obs}/C_i \quad (4)$$

Stokes and Anti-Stokes Raman Spectral Profiles. Using these assumptions and considerations, we determined the Boltzmann temperatures of the solvent (T_{835}) using eq 2 for dioxane solutions of (L_nTPP)Fe(III)Cl ($n = 3$ to 5) as well as neat solvent after calculating the $(I_S/I_{AS})_T$ from the observed $(I_S/I_{AS})_{obs}$ values of the 835-cm^{-1} band in the presence and absence of the IR band-pass filter. The Boltzmann temperature for the neat solvent with IR irradiation at 80 V without the IR filter was 294.1 ± 0.6 K, indicating no direct heating effect by the ceramic heater. Figure 7 shows the Boltzmann temperatures of solvent plotted against the voltage applied to the ceramic heater. The values contain the contribution of heating (1.5 K) by the Raman excitation light at 3 mW. The error bars represent the magnitude of data scattering in three, three, and two independent measurements for L_3, L_4, and L_5 samples, respectively, and are expected to involve the contributions from errors in C_i. The temperature thus obtained in the absence of IR illumination (at 0 V of applied voltage) was the same as the environment temperature (295.7 K). It is clear that, at a designated voltage (55−90 V) applied to the ceramic heater and under otherwise identical conditions, the Boltzmann temperature of the solvent in the absence of an IR band-pass filter is slightly higher than that in the presence of the filter. On the other hand, in both cases, the Boltzmann temperature of the solvent showed a similar tendency to increase with the intensity of IR illumination, and the maximum temperature increase of the solvent upon IR illumination was 5 K at a voltage of 90 V in the absence of the IR band-pass filter. Since the temperature increase of neat solvent under the same irradiation condition was negligible, the temperature increase of the solvent is mainly due to the vibrational energy relaxation of the excited antenna molecules in the solution. This inference is reasonable because the temperature increments are diminished in the presence of the IR band-pass filter compared to its absence. The temperature increments of the solvent did not differ greatly among solutions of (L_nTPP)Fe(III)Cl with different numbers of aryl ether layers. However, the temperature rise of the solvent observed in the presence of the IR band-pass filter supports the concept of IR energy capturing by vibrational modes of the aryl units, which could also transfer the captured energy to the solvent.

Evaluation of Boltzmann Temperatures. To determine whether the captured energy is transferred to the chloroiron(III) porphyrin unit located at the center of (L_nTPP)Fe(III)Cl ($n = 3$ to 5), the Boltzmann temperatures of two porphyrin bands [390 (T_{390}) and 355 cm^{-1} (T_{355})] were determined in the same way as for the solvent. To eliminate a possible contribution from heating effects by other sources, the results were examined in the form of differential temperatures by subtracting the Boltzmann temperature of the solvent (T_{835}) from T_{390} and T_{355}: $\Delta T_{355} = T_{355} - T_{835}$ and $\Delta T_{390} = T_{390} - T_{835}$. Figures 8 and 9 show the plots of ΔT_{355} and ΔT_{390} versus the voltage applied to the ceramic heater, which were measured in the presence and

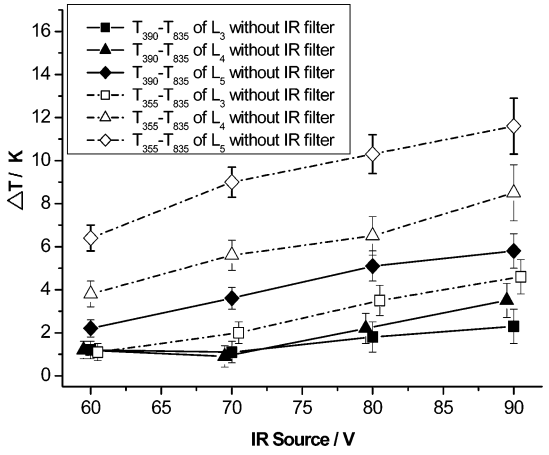

Figure 9. Dependence of the Boltzmann temperatures ΔT_{390} ($T_{390} - T_{835}$) and ΔT_{355} ($T_{390} - T_{835}$) of (L_nTTP)Fe(III)Cl/dioxane solution on the voltage applied to the IR source in the absence of an IR band-pass filter at an environmental temperature of 295.7 K. The complete sets of independent measurements were carried out three, three, and two times for L_3, L_4, and L_5 samples, respectively. The error bars were determined from the scattering of the data.

absence of the IR band-pass filter, respectively. We found the following general trends:

(1) All of the ΔT_{355} and ΔT_{390} values are positive, suggesting that the Boltzmann temperatures of the solute (T_{390} and T_{355}) are higher than that of the solvent (T_{835}).

(2) The ΔT_{355} and ΔT_{390} values show a weak but clear tendency to increase with the voltage applied to the ceramic heater.

(3) At a designated voltage applied to the ceramic heater, the ΔT_{355} and ΔT_{390} values increase with the number of the aryl ether layers (n) of the dendrimer framework.

(4) For each dendrimer chloroiron(III) porphyrin complex, the temperature rise for the Fe−Cl stretching mode is always higher than that for the porphyrin ν_8 mode ($\Delta T_{355} > \Delta T_{390}$), regardless of whether it is measured in the presence or absence of the IR band-pass filter.

(5) The difference between ΔT_{355} and ΔT_{390} enlarges when the generation of the dendrimer framework is increased.

(6) The ΔT_{355} and ΔT_{390} values in the presence of the band-pass filter are smaller than those evaluated in the absence of the filter. However, the proportion of reduction is compatible with the idea that IR energy is primarily captured by the aryl ν_8 vibration of the dendrimer framework as discussed below quantitatively. The maximum values of ΔT_{355} observed for (L_5-TPP)Fe(III)Cl in the presence and absence of the filter were 7.3 and 11.6 K, respectively.

Mechanistic Aspects. These findings indicate that the aryl ether dendrimer framework in (L_nTPP)Fe(III)Cl absorbs IR photons through the phenyl ν_8 mode at 1597 cm^{-1} and transfers their energy to the central porphyrin unit. As shown in Figure 1, larger dendrimers contain an increased number of aryl units in their framework. Therefore, this property is in good agreement with the results from the harvesting of IR photons through the aryl units, as demonstrated by the dendrimer size effect; specifically, (L_nTPP)Fe(III)Cl with a large dendrimer framework has a large temperature increase that is even greater under high-intensity IR illumination.

From the general viewpoint of vibration-to-vibration resonance energy transfer, the vibrational quantum excited in the aryl units may be transferred to the porphyrin ring mode with the closest frequency, such as the one at 1555 cm^{-1} (see Figure 4). However, as noted for Figures 5 and S3, there was no anti-Stokes band observed in the region from 1500 to 1650 cm^{-1}. Instead, we observed the anti-Stokes bands for the axial Fe−Cl stretching and porphyrin in-plane vibrational modes at 355 and 390 cm^{-1}, respectively. The mode dependency of the temperature increase ($\Delta T_{355} > \Delta T_{390}$) is compatible with the idea that the vibrational energy captured by the dendrimer framework is transferred to the axial position of the core porphyrin unit first and then promptly relaxed to in-plane vibrational modes. Because the vibrational energy redistribution finishes within a few picoseconds for metalloporphyrins,[14] the temperatures of the Fe−Cl stretching and porphyrin in-plane vibrational modes are usually the same when the IR pumping rate is slower than the rate of vibrational energy redistribution in the photo steady-state measurements. Furthermore, the Boltzmann temperatures of the solute should be the same as that of the solvent if intermolecular vibrational energy transfer is faster than the IR pumping rate ($\Delta T = 0$). Interestingly, both ΔT_{355} and ΔT_{390} are positive, meaning that the observed temperature changes are caused by some systematic process, and the ΔT_{355} thus obtained is still larger than ΔT_{390} (7.5 versus 3.8 K in the presence of the IR filter and 11.5 versus 5.7 K in the absence of the IR filter). The difference between ΔT_{355} and ΔT_{390} would be much larger if picosecond time-resolved Raman measurements were performed using a picosecond IR pump source.

The proportion of reduction of ΔT by the IR filter is 65% (= 7.5/11.5) and 67% (= 3.8/5.7) for the 355 and 390 cm^{-1} bands, respectively. These values happen to be very close to the value of transmittance of the IR filter at 1597 cm^{-1} (70.05%). Since the ν_8 IR absorption of the dendrimer framework has some width and the transmittance of the filter changes with the frequency, the precise estimation of the expected value is not straightforward. However, it can be concluded that other dendrimer modes (such as CH_2−O str. at 1155 cm^{-1}) do not play a larger role in the heating. If the CH_2−O mode were involved, the measurements with the filter should include the contribution of removing this large absorber, and thus the ΔT change should be much greater than 65%. Consequently, the present observations strongly suggest that IR energy contributing to temperature rise of the core porphyrin is mainly captured by the ν_8 mode of the dendrimer faramework. Such a trend is observed for all members of the (L_nTPP)Fe(III)Cl family.

On the other hand, if the phenyl ν_8 mode (1597 cm^{-1}) of the dendrimer framework is specifically excited by IR irradiation and its vibrational relaxation is relatively slow, its anti-Stokes Raman band is expected to appear at 1597 cm^{-1}. Therefore, we attempted to find an anti-Stokes band under IR irradiation in the region between 1500 and 1650 cm^{-1}. However, as described earlier (Figures 5 and S3), we failed to detect a trace of such a peak in this frequency region, even upon IR irradiation at a voltage of 80 V applied to the ceramic heater. These results indicate that the vibrational energy transfer from the aryl dendritic antenna to the core porphyrin unit must be extremely fast.

The fact that ΔT_{355} exceeded ΔT_{390} for all independent measurements leads us to conclude that the IR energy captured by the aryl dendritic antenna is accumulated on the axial ligand

position of the central chloroiron(III) porphyrin unit. At present, we cannot explain why this occurs, although we note that this observation is consistent with the IR-induced cleavage of the axial ligand of oxygenated dendrimer iron(II) porphyrin complex.[10] Further study is necessary to unravel this process. Such an accumulation feature was thought unusual at that time, but as demonstrated in this study, it was confirmed by a quite different technique, that is, the direct measurement of temperature at the reaction point under IR irradiation. The difference between ΔT_{355} and ΔT_{390} increases with increasing dendrimer size while both the ΔT_{355} and ΔT_{390} values become larger, presumably because the more confining environment around the axial Fe−Cl bond in a larger dendrimer would protect the energy transfer from collision scattering and would insulate the Fe−Cl bond from thermal perturbation. This, in turn, would suppress the vibrational energy relaxation to the porphyrin macrocycle.

Conclusions

By using anti-Stokes Raman spectroscopy, we determined the Boltzmann temperatures of (L_nTPP)Fe(III)Cl in dioxane for two vibrational bands of the central chloroiron(III) porphyrin functionality under variable intensity IR illumination. The Boltzmann temperatures of (L_nTPP)Fe(III)Cl modes (390 and 355 cm^{-1}) were higher than that of the solvent (835 cm^{-1}), while the temperature of neat solvent (835 cm^{-1}) was unaffected, and the temperature rise was greater for dendrimers with a large framework and increased with increasing IR intensity. Between the two porphyrin vibrational modes with similar frequencies, the Fe−Cl stretching mode was more heated than an in-plane mode of the porphyrin macrocycle. On the other hand, the proportion of reduction of the temperature rise by the IR filter was in agreement with the transmittance of IR light at 1597 cm^{-1}. This indicates that the energy of IR photons captured mainly by the ν_8 mode of the aryl dendritic antenna is transferred to the axial position of iron and subsequently relaxed to the porphyrin macrocycle. Thus, the present study not only demonstrates a new IR illumination effect on dendrimer metalloporphyrins but also provides a novel approach to evaluate IR energy funneling in light-harvesting dendritic macromolecules.

Acknowledgment. We thank Prof. Hiroshi Fujii of the Okazaki Institute for Integrative Bioscience, Japan, for his help in the preparation of (TPP)Fe(III)Br, and Dr. Hirotsugu Hiramatsu of this laboratory for determining the transmittance spectrum of the IR filter. This work was supported by a Grant-in-Aid for Specifically Promoted Research from the Ministry of Education, Culture, Sports, Science, and Technology, Japan, to T.K. (14001004).

Supporting Information Available: Relative emission intensity of the ceramic heater in the 4000 to 0 cm^{-1} region when AC 100 V is applied, which was observed with a Jasco FT/IR-6000 (vacuum type) (Figure S1), the transmission spectrum of the IR filter in the wavenumber range between 8000 and 350 cm^{-1}, in which the inset represents the expanded spectrum between 2000 and 400 cm^{-1} (Figure S2), and anti-Stokes resonance Raman spectra of L_4(TPP)Fe(III)Cl in dioxane in the absence of an IR band-pass filter with a voltage applied to the IR source at (a) 0 V and (b) 80 V at an environmental temperature of 295.7 K and excitation by a Kr^+ ion laser at 413.1 nm with a power of 3 mW (Figure S3). This material is available free of charge via the Internet at http://pubs.acs.org.

JA042196Z